# Dirac fermion tunneling current through thin $MoS_2$ insulating barriers: Novel utilities of graphene heterostructures

Nojoon Myoung,[1] Kyungchul Seo,[1] Seung Joo Lee,[2] and Gukhyung Ihm[1]

[1] *Department of Physics, Chungnam National University, Daejeon 305-764, Korea*

[2] *Quantum-functional Semiconductor Research Center, Dongguk University, Seoul 100-715, Korea*

(Dated: February 6, 2013)

**Graphene has been considered to be a promising material for future electronics due to its extraordinary properties such as high carrier mobility[1, 2], thermal conductivity[3], and strong break strength[4]. Although the extremely high electrical conductivity makes graphene a candidate for replacing silicon-based electronics, Klein tunneling causes that electrical transport of Dirac fermions is insensitive to electrostatic potentials, resulting a low current on/off ratio of graphene-based field effect transistors[5–7]. In order to increase the current on/off ratio, vertical graphene heterostructures have been introduced as an alternative device architecture[8, 9], by using quantum tunneling. Here, in addition to the experimental observations which gave us a large current on/off ratio of graphene/$MoS_2$ heterostructures, we present that the current on/off ratio is enhanced by as large as two orders of magnitude compared to the previous report[8]. Moreover, we also report a novel utility of the graphene/$MoS_2$ heterostructures as a spin-filter. When a thin $MoS_2$ layer sandwiched between two graphene sheets becomes magnetic because of the inversion symmetry breaking[10], Dirac fermions with different spins feel different heights of a tunnel barrier, resulting spin-dependent tunneling. Our findings will develop the present graphene heterostructures for electronic devices by improving the device performance and by adding the functionality to the existing graphene heterostructures.**

Very recently, increasing interest has been focussed on an alternative graphene device structure by using quantum tunneling. In a graphene/silicon junction, large current on/off ratio was achieved by controlling the Schottky barrier at the interface[11]. However, for graphene deposited on silicon substrate, carrier mobility is expected to decrease because of carrier inhomogeneity induced by the substrate[12]. Meanwhile, L. Britnell et al. reported the possibility of a graphene field-effect-transistor based on vertical heterostructures with atomically thin insulating barriers, hexagonal boron nitride ($h$BN) and molybdenum disulfide ($MoS_2$)[8]. $h$BN has gained burgeoning interest as a material for use in graphene devices because the encapsulation of graphene by $h$BN maintains the high electronic quality of pristine one[13–15]. In spite of this advantage, the large band gap of $h$BN ($\sim 5.97\ eV$[16]) causes an insufficient current on/off ratio. Instead of $h$BN, the larger on/off ratio was observed in graphene heterostructure with $MoS_2$, owing to its smaller bandgap than $h$BN. Therefore, the

graphene heterostructure with $MoS_2$ can be an important building block of graphene-based electronics, and it is natural to investigate possible functional devices utilizing its advantages for applications.

Herein, we present not only the improvement of the current on/off ratio of the existing graphene/$MoS_2$ heterostructures[8] but also an application of the heterostructure in spintronics by producing spin-dependent transport. First, we show that there emerge current peaks for a graphene/$MoS_2$/grarphene nanoribbon (GNR) heterostructure. This finding has potential for the use of the current peaks, resulting in the improvement of the current on/off ratio. Second, the existence of magnetic properties in few-layer $MoS_2$[17–22] can lead to the spin-polarized current in the graphene heterostructures. We show that the graphene heterostructure can be a perfect spin-filter for holes with the electron-hole asymmetric spin splitting of $MoS_2$[10]. Such tunneling phenomena may offer further potential applications in graphene-based electronics and spintronics.

Now, we consider a heterostructure, which consists of an atomically thin $MoS_2$ layer sandwiched by two graphene sheets as shown in Fig. 1a. It is well known that few-layer $MoS_2$ is an insulator with finite bandgaps; $\sim 1.9\ eV$ direct bandgap near the K-valley and $\sim 1.2 - 1.4\ eV$ indirect bandgap depending on the number of $MoS_2$ layers[23]. The $MoS_2$ layer of the heterostructure becomes a tunnel barrier for Dirac fermions, and both graphene sheets play the role of high-quality source and drain electrodes. Dirac fermions experience the direct bandgap near K-valley of $MoS_2$ because of the momentum conservation, neglecting electron-phonon scattering processes.

We can obtain the tunneling current through the $MoS_2$ insulating barrier as below

$$j\left(V_b, V_G\right) = j_0 \int_{-\infty}^{+\infty} D_S\left(E, V_b\right) D_D\left(E, V_b\right) T\left(E\right) \left[f_S\left(E, V_b, V_G\right) - f_D\left(E, V_b, V_G\right)\right] dE, \quad (1)$$

where $j_0 = \left(q v_F\right) / \left(2\pi L_0^3\right)$ is the unit of current density with electric charge of carriers, $q$, and the characteristic length of the system, $L_0$. We can calculate the transmission probability, $T\left(E\right)$, with a quantum-mechanical consideration (see Supplementary Information). Here, $D_i$ and $f_i$ are density of states of graphene and the Fermi-Dirac distribution where $i = S,\ D$ represent source and drain graphene electrodes on both sides of the $MoS_2$ layer, respectively. We assume that the gate voltage induces the equal carrier concentration in both graphene sheets; $n = \alpha V_g$ where $\alpha = 6.16 \times 10^{14}\ Cs^2kg^{-1}m^{-4}$ in a case of a 300 $nm$ thick $SiO_2$ substrate. For a given $V_g$, chemical potentials in both graphene sheets are equally

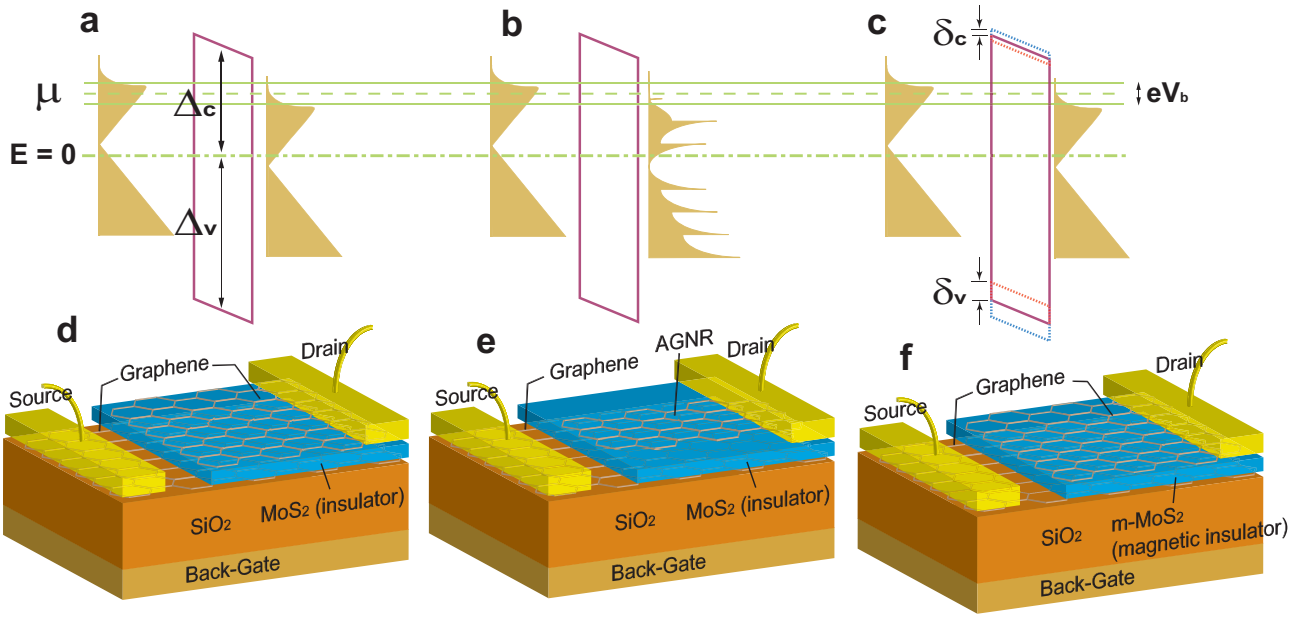


FIG. 1. **Graphene heterostructures with $MoS_2$ thin layers.** **a**, **b**, **c**, Each panel shows energetic diagrams for quantum tunneling through $MoS_2$ insulating barriers for different heterostructures; graphene/$MoS_2$/graphene, graphene/$MoS_2$/AGNR, and graphene/m-$MoS_2$/graphene. Since the charge neutral point of graphene is asymmetrically laid, electrons and holes experience different tunnel barriers, $\Delta_c$ and $\Delta_v$, respectively. **b**, If one graphene electrode is replaced by a narrow GNR, density of states is changed, showing the one-dimensional nature. **c**, When the $MoS_2$ is magnetic, the barrier height becomes spin-dependent, with different spin-splitting energies $\delta_c$ and $\delta_v$. **d**, **e**, **f**, Schematic diagrams of different heterostructures corresponding to **a**, **b**, **c**, respectively. $MoS_2$ is sandwiched by two graphenes which act as source and drain electrodes. The equilibrium chemical potential, $\mu_0$, is induced via back gate, and the tunneling current is generated by source-drain bias voltage, $V_b$.

given as $\mu = \hbar v_F \sqrt{\pi |n|} = \hbar v_F \sqrt{\pi \alpha |V_g|}$. The equal chemical potentials produce no net tunneling current through the $MoS_2$ barrier. Applying the bias voltage, $V_b$, between the source and drain graphene electrodes, one can measure non-zero tunneling current through the heterostructure.

Figure 2 displays the characteristics of the graphene/$MoS_2$/graphene heterostructure. The calculated tunneling currents as functions of $V_b$ for different $V_g$ are shown in Fig. 2a. The tunneling current exhibits an exponentially increasing behaviour and becomes larger as $V_g$ increases because more carriers contribute to the quantum tunneling for high $V_g$. The

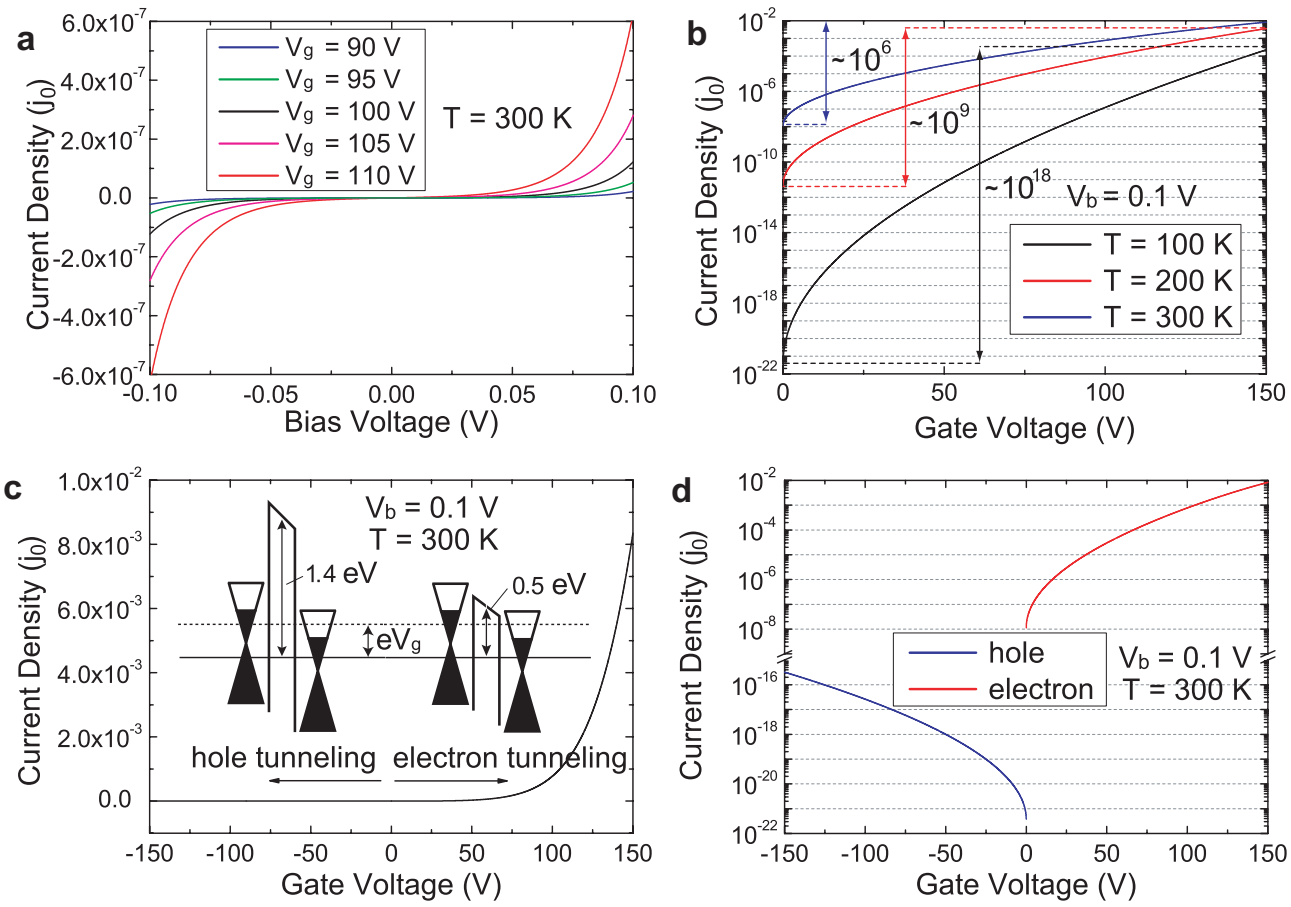


FIG. 2. **I-V characteristics of graphene/$MoS_2$/graphene heterostructure.** **a**, Tunneling current densities as functions of bias voltage for different gate voltages at 300 $K$. **b**, Temperature dependence of the tunneling current densities. Tunneling current densities are plotted in logarithmic scale as functions of gate voltage for the given bias voltage, $V_b = 0.1\ V$. **c**, Asymmetric tunneling current density curve versus gate voltage at 300 $K$ for the given bias voltage, $V_b = 0.1\ V$. (Inset) Energetic diagrams for electron and hole tunnelings. Electrons and holes are induced by applying the gate voltage, $V_g$. **d**, Log-linear curves of the electron and hole tunneling current densities as a function of gate voltage at 300 $K$ for the given bias voltage, $V_b = 0.1\ V$. In spite of different magnitudes of the current densities between electrons and holes, we can obtain similar current on/off ratios about $10^6$. A parameter $j_0 = (qv_F) / \left(2\pi L_0^3\right)$ in use is the unit of current density.

tunneling current versus gate voltage curves are plotted in Fig. 2b. We find the ratio of the tunneling current between an off-state ($V_g = 0\ V$) and an on-state ($V_g = 150\ V$) at different temperatures. With increasing temperature, the magnitude of tunneling current correspond-

ingly increases because more carriers are thermally activated, but the current on/off ratio decreases. While the current on/off ratio reaches up to $10^{18}$ at 100 $K$, it goes down to $10^6$ at 300 $K$. Despite of this decrease, the room-temperature current on/off ratio is still high as experimentally expected in Ref. 18. This means that the graphene/$MoS_2$/graphene heterostructure can be a platform for graphene-based field-effect transistors.

For graphene/$MoS_2$ hybrid systems, the charge neutral point of Dirac cone is asymmetrically arranged between the conduction and valence bands near K-valley of $MoS_2$[21]. Thus, electrons experience a lower tunnel barrier ($\Delta_c \simeq 0.5\ eV$) than holes ($\Delta_v \simeq 1.4\ eV$), where $\Delta_c$ and $\Delta_v$ are the barrier heights for electrons and holes, respectively. If the tunneling electrons and holes have the same energy, the transmission probability through the $MoS_2$ insulating barrier for electrons is greater than for holes because electrons experience the smaller tunnel barrier than holes. Figure 2c exhibits the difference between electron and hole tunneling currents as functions of gate voltage. We found that the tunneling current is indeed asymmetric with respect to the gate voltage polarity. However, as shown in Fig. 2d, the on/off ratio of electron and hole tunneling currents is about the same although the hole tunneling current is suppressed.

Next, we can enhance the current on/off ratio of the graphene/$MoS_2$/graphene heterostructure by considering size effects of a graphene electrode. In order to study the size effects, we replace a graphene electrode on one side of the sandwiched $MoS_2$ layer with a GNR as shown in Fig. 1b. Because the tunneling current density depends on the product of densities of states of source and drain graphene electrodes, (Eq. (1)), one can expect the changes in the tunneling current. In this letter, we take into account a graphene nanoribbon with armchair edges (AGNR) of which the density of states exhibits the one-dimensional nature (see Supplementary Information).

The resulting tunneling currents through a graphene/$MoS_2$/AGNR heterostructure are plotted in Fig. 3a as functions of $V_b$ for different $V_g$. There emerge tunneling current peaks at specific $V_b$ because of the one-dimensional nature of the AGNR. This feature of the graphene/$MoS_2$/AGNR heterostructure plays a crucial role in the enhancement of the current on/off ratio. Figure 3b shows log-linear plots of the tunneling current densities as functions of $V_g$ for different $V_b$. The magnitude of the currents at a current peak (for $V_b \simeq 0.1\ V$, blue lines) is about $10^2$ times larger than the background values (for $V_b \simeq 0.11\ V$, red lines). If one vary $V_b$ from $\simeq 0.11\ V$ to $\simeq 0.1\ V$ simultaneously with adjusting $V_g$, one

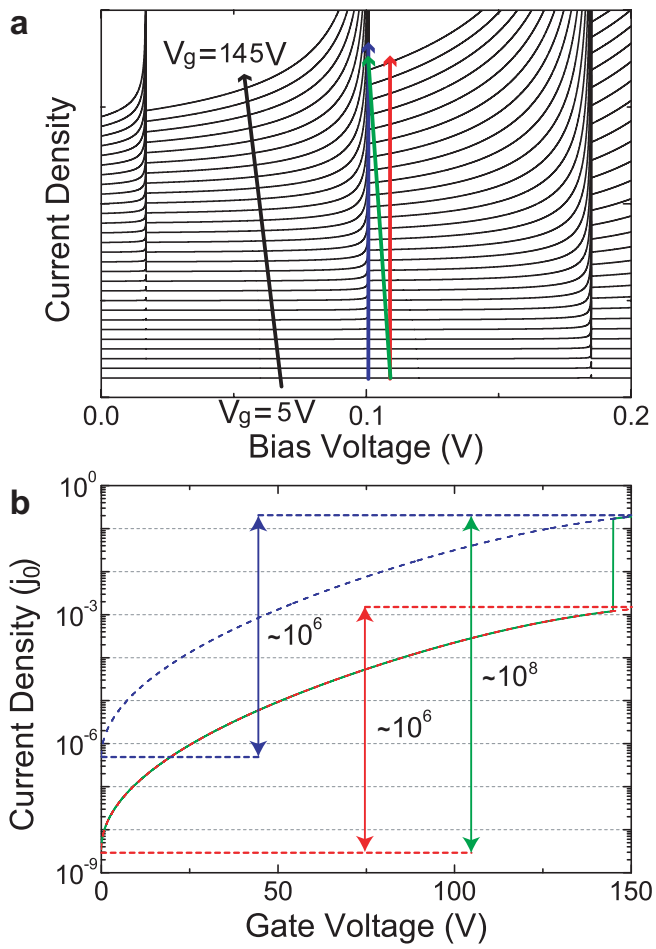


FIG. 3. **I-V characteristics of graphene/$MoS_2$/AGNR heterostructures.** **a**, Tunneling current densities through a graphene/$MoS_2$/AGNR heterostructure as functions of bias voltage for different gate voltages (arbitrary units). Some current peaks emerge at the specific bias voltages due to the one-dimensional nature of AGNRs. **b**, Comparison of the current on/off ratios in different cases; blue, red, and green solid lines depicted in **a**. Blue and red dashed curves indicate the current density versus the gate voltage for different fixed bias voltages, $V_b \simeq 0.1\ V$ and $0.11\ V$, respectively. Green solid curve shows the current density as a function of gate voltage, varying simultaneously bias voltage from $0.11\ V$ to $0.1\ V$.

can obtain an abrupt jump in the tunneling current density as large as $10^2$ (green lines). Due to the existence of the current peak, there emerges an abrupt jump of the current density as large as $10^2$, and the resulting current on/off ratio is enhanced up to $10^8$. Therefore, the use of an AGNR instead of a graphene electrode is attractive for applications in graphene-based electronics, improving the performance of the graphene heterostructures with $MoS_2$ layers.

In recent years, it was found to exhibit magnetic properties in an atomically thin $MoS_2$ layer due to several causes; sulfur-vacancy or zigzag-terminated grain boundary[10, 17–22]. For instance, the broken inversion symmetry due to the sulfur-vacancy leads to a splitting between different spin states for few-layer $MoS_2$, but there is no spin-splitting for bulk $MoS_2$[10]. This allows us to assume that the $MoS_2$ layer used in our heterostructures is thin enough to have a non-zero spin-splitting energy. In this case, the thin $MoS_2$ layer can be treated as a magnetic insulator with spin-dependent barrier heights, $U(z) = \Delta + \sigma\delta_{c,v} + (qV_b z/d)$ where $\sigma = \pm$ represents different spins and $\delta_{c,v}$ indicate spin-splitting energies in the conduction and valence bands of $MoS_2$, respectively. We focus on the spin-splitting near K-valley of $MoS_2$ because tunneling Dirac fermions experience the direct bandgap near K-valley of $MoS_2$, as aforementioned.

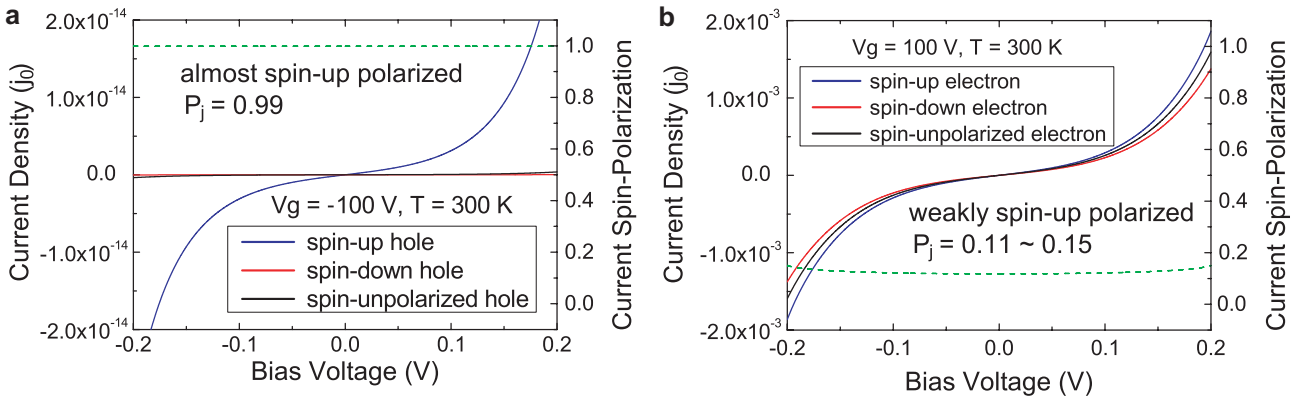


FIG. 4. **Graphene/m-$MoS_2$/graphene as a spin-filter for hole tunneling.** Spin-dependent current density for **a**,**b**, electron and hole tunneling, respectively.through a graphene/m-$MoS_2$/graphene heterostructure. Both panels exhibit spin-unpolarized currents (blue solid lines) in comparison with spin-dependent currents. Black and red solid lines indicate tunneling current densities for spin-up and down carriers, respectively. Green dashed lines represent the spin-polarization of tunneling current densities.

Our results of spin-dependent tunneling currents through a magnetic $MoS_2$ (m-$MoS_2$) are shown in Fig. 4 for different kinds of carriers, electrons and holes. Here, the spin-polarization of tunneling current is calculated as $P_j = (j_{up} - j_{down}) / (j_{up} + j_{down})$. In Fig. 4, one can see the differences in the spin-dependent features between electron and hole tunneling currents. While the hole tunneling current is almost perfectly spin-polarized, the electron tunneling current is weakly spin-polarized. This is due to the fact that the spin-splitting in the valence

band is about 50 times larger ($\delta_v \simeq 150\ meV$) than the conduction band ($\delta_c \simeq 3\ meV$)[10]. The small spin-splitting energy near K-valley in the conduction band leads to the weak spin-polarization of the electron tunneling current; $P_j = 0.11 - 0.15$. Meanwhile, due to the large spin-splitting near K-valley in the valence band, the hole tunneling current is almost perfectly spin-polarized, $P_j = 0.99$. Thus, the graphene/m-$MoS_2$/graphene heterostructures provide a potential application in spintronic devices as a good spin filter.

In summary, we have investigated the characteristics of the tunneling current through the graphene heterostructures with thin $MoS_2$ layers. We have done calculations for various heterostructures; graphene/$MoS_2$/graphene, graphene/$MoS_2$/AGNR and graphene/m-$MoS_2$/graphene. We show that the current on/off ratio of graphene/$MoS_2$/graphene is up to $10^6$ at room temperature. We also find that the graphene/$MoS_2$/graphene heterostructure exhibits the carrier-dependent tunneling phenomena, which allows electrons to tunnel through the heterostructure, more easily than holes. Furthermore, we show that the current on/off ratio can be enhanced up to $10^8$ by replacing a two-dimensional graphene electrode with a GNR electrode. Finally, we propose a novel utility, the spin-polarized tunneling current, in the case that there is the splitting between different spin states in the thin $MoS_2$ layer. We show that the different spin-splitting energy between the conduction and valence bands of $MoS_2$ makes the hole tunneling current almost perfectly spin-polarized whereas the electron tunneling current is partially spin-polarized. The graphene/m-$MoS_2$/graphene heterostructure may acts as a spin-filter for holes, which is a crucial building block of future spintronic devices. Our findings may not only offer an advance in research on the vertical graphene heterostructures with atomically thin insulating layers but also contribute to graphene-based spintronics.

**ACKNOWLEDGMENT**

This work was supported by Basic Science Research Program through the NRF funded by the Ministry of Education, Science, and Technology(2012R1A1A4A01008299,NO2012R1A1A2005772).

## AUTHOR CONTRIBUTION

N.M. performed most of the calculations and mainly analyzed the results with in-depth discussions with K.S., S.J.L. and G.I. All the authors contributes to the writing of the manuscript.

## COMPETING FINANCIAL INTERESTS

The authors declare no competing financial interests.

## CORRESPONDING AUTHOR

Correspondence to G. Ihm or S. J. Lee

---

[1] Novoselov, K. S. et al. Two-dimensional gas of massless Dirac fermions in graphene. Nature **438**, 197 (2005).

[2] Zhang, Y., Tan, Y.-W., Stormer, H. L. & Kim, P. Experimental observation of the quantum Hall effect and Berry's phase in graphene. Nature, **438**, 201 (2005).

[3] Ghosh, S. et al. Dimensional crossover of thermal transport in few-layer graphene. Nat. Mater. **9**, 555 (2010).

[4] Lee, C., Wei, X. D., Kysar, J. W. & Hone, J. Measurement of the elastic properties and intrinsic strength. Science **321**, 385 (2008).

[5] Wu, Y. et al. High-frequency, scaled graphene transistors on diamond-like carbon. Nature **472**, 74 (2011).

[6] Liao, L. et al. High-speed graphene transistors with a self-aligned nanowire gate. Nature **467**, 305 (2010).

[7] Han, S. J. et al. High-frequency graphene voltage amplifier. Nano Lett. **11**, 3690 (2011).

[8] Britnell, L. et al. Field-effect tunneling transistor based on vertical graphene heterostructures. Science **335**, 947 (2012).

[9] Yu, W. J. et al. Vertically stacked multi-heterostructures of layerd materials for logic transistors and complementary inverters. 10.1038/nmat3518.

[10] Kadantsev, E. S. & Hawrylak, P. Electronic structure of a single $MoS_2$ monolayer. Solid State Commun. **152**, 909 (2012).

[11] Yang, H. et al. Graphene barristor, a triode device with a gate-controlled Schottky barrier. Science **336**, 1140 (2012).

[12] Sabio, J. et al. Electrostatic interactions between graphene layers and their environment. Phys. Rev. B **77**, 195409 (2008).

[13] Dean, C. R. et al. Boron nitride substrates for high-quality graphene electronics. Nat. Nanotechnol. **5**, 722 (2010).

[14] Giovannetti, G., Khomyakov, P. A., Brocks, G., Kelly, P. J. & D. Brink, J. V. Substrate-induced band gap in graphene on hexagonal boron nitride: ab initio density functional calculations. Phys. Rev. B **76**, 073103 (2007).

[15] Mayorov, A. S. et al. Micrometer-scale ballistic transport in encapsulated graphene at room temperature. Nano Lett. **11**, 2396 (2011).

[16] Zhao, J., Yu, Y., Bai, Y., Lu, B. & Wang, B. Chemical functionalization of BN graphene with the metal-arene group: a theoretical study. J. Mater. Chem. **22**, 9343 (2012).

[17] Li, Y., Zhou, Z., Zhang, S. & Chen, Z. $MoS_2$ nanoribbons: high stability and unusual electronic and magnetic properties. J. Am. Chem. Soc. **130**, 16739 (2008).

[18] Ataca, C., Şahin, H., Aktürk, E. & Ciraci, S. Mechanical and electronic properties of $MoS_2$ nanoribbons and their defects. Phys. Chem. C **115**, 3934 (2011).

[19] Wang, Z., et al. Mixed low-dimensional nanomaterial: 2D ultranano $MoS_2$ inorganic nanoribbons encapsulated in quasi-1D carbon nanotubes. J. Am. Chem. Soc. **132**, 13840 (2010).

[20] Botello-Méndez, A. R., López-Urías, F., Terrones, M. & Terrones, H. Metallic and ferromagnetic edges in molybdenium disulfide nanoribbons. Nanotechnol. **20**, 325703 (2009).

[21] Shidpour, R. & Manteghian, M. A density functional study of strong local magnetism creation on $MoS_2$ nanoribbon by sulfer vacancy. Nanoscale **2**, 1429 (2010).

[22] Tongay, S., Varnoosfaderani, S. S., Appleton, B. R., Wu, J. & Hebard, A. F. Magnetic properties of $MoS_2$: Existence of ferromagnetism. Appl. Phys. Lett. **101**, 123105 (2012).

[23] Mak, K. F., Lee, C., Hone, J., Shan, J. & Heinz, T. F. Atomically thin $MoS_2$: A new direct band-gap semiconductor. Phys. Rev. Lett. **105** 136805 (2010).